

## Ion-induced electron-emission study of high- $T_c$ superconductors and phase transitions

Hermann Rothard,\* Markus Schosnig, Kurt Kroneberger, and Karl-Ontjes Groeneveld  
*Institut für Kernphysik der J. W. Goethe-Universität, August-Euler-Strasse 6, D-6000 Frankfurt-am-Main 90,  
 Federal Republic of Germany*

(Received 18 November 1991; revised manuscript received 24 March 1992)

We have investigated the phenomenon of kinetic ion-induced electron emission from high-temperature copper oxide superconductors. The total yield  $\gamma_T$  of electrons induced by  $H^+$  and  $Ar^+$  (0.8 MeV) from polycrystalline  $YBa_2Cu_3O_{7-\delta}$  has been measured as a function of the probe temperature ( $70\text{ K} \leq T \leq 300\text{ K}$ ). It shows a minimum close to the superconducting phase-transition temperature of  $T_C \approx 93\text{ K}$ . Electron-energy distributions ( $0\text{ eV} \leq E \leq 40\text{ eV}$ ,  $25^\circ \leq \theta \leq 90^\circ$ ) from  $H^+$ - and  $C^+$ - (2-MeV) bombardment of single crystals of  $YBa_2Cu_3O_{7-\delta}$  and  $EuBa_2Cu_3O_{7-\delta}$  high- $T_C$  superconductors show the low-energy peak of "true secondary electrons" at  $E_{\max} \approx 5\text{ eV}$  and in the case of  $YBa_2Cu_3O_{7-\delta}$  a further weak structure at  $E \approx 14\text{ eV}$ , which can possibly be attributed to Auger electron emission from yttrium. The electron angular distributions  $N(\theta)$  have been measured at sample temperatures above ( $T = 300\text{ K}$ ) and below ( $T = 35\text{ K}$ ) the superconducting transition temperature ( $T_C \approx 90\text{ K}$ ) as a function of the angle of incidence ( $\delta = 55^\circ, 65^\circ, 70^\circ, 75^\circ$ ) of the projectiles. The ratio  $R = N(C^+)/N(H^+)$  of electron intensities from heavy  $C^+$  ion impact to the electron intensities from proton impact shows broad peaks ( $\Delta\theta \approx 25^\circ$ ) at low electron energies  $E < 20\text{ eV}$ . The mean emission angle  $\theta_{em}$  of the excess electrons belonging to this peak shifts to higher angles  $\theta$  with increasing  $\delta$ . This can be explained by the directed emission of so-called "shock electrons" perpendicular to the conical charge density fluctuations ("wake") caused by the ion. The experimental results are in agreement with calculations within the framework of a simple model, which takes into account the refraction of low-energy electrons at surfaces, as well as the electronic structure of the copper oxide superconductors. They are characterized by two different collective excitation frequencies, i.e., the plasma frequency  $\omega_p^{FC}$  of the free charge carriers (O 2p holes) ( $\hbar\omega_p^{FC} \approx 1.5\text{ eV}$ ) and the volume plasma frequency  $\omega_p^{VP}$  of the collective excitation of all the electrons in one unit cell of the crystals ( $\hbar\omega_p^{VP} \approx 25\text{ eV}$ ). Finally, the influence of magnetic and structural phase transitions and, in particular, the superconducting phase transition at  $T = T_C$  on ion-induced electron emission from solids is discussed.

### I. INTRODUCTION

Experimental studies of the phenomenon of kinetic ion-induced electron emission from solids are important not only for many practical applications, but also for our basic understanding of the interaction of ionizing radiation with condensed matter, compare e.g., Ref. 1. An interesting fundamental experiment on electron emission is the measurement of (observation angle and energy integrated) electron yields,  $\gamma_F$  and  $\gamma_B$ , from the entrance and the exit surfaces of thin foils as a function of the projectile nuclear charge  $Z_p$ , the target material  $Z_T$ , and the projectile velocity  $v_p$ . Also, it is interesting to measure electron yields  $\gamma$ , i.e., the mean number of ejected electrons per projectile, from thick samples in backward direction only. For a detailed discussion of recent results from such measurements, the reader is referred to Ref. 1. Even more information can be obtained by measuring the (angle-integrated) energy distribution  $N(E)$ , the (energy-integrated) angular distribution  $N(\theta)$ , or even the observation angle ( $\theta$ ) dependence of doubly differential electron energy spectra  $d^2n/dE_e d\Omega$ .<sup>1</sup>

The interaction of swift (MeV) ions with solids causes a dynamical collective response of the electron plasma ("wake").<sup>1-5</sup> The term "wake" was introduced by Niels Bohr in his famous paper on "the penetration of charged

particles through matter" in 1948 (Ref. 2) probably because the spatial structure of the ion-induced polarization somewhat resembles a ship's wake in water. These conical electron density fluctuations show the characteristic behavior of Mach shock waves and lead to the directed emission of shock electrons perpendicular to the wake shock front.<sup>1,3-9</sup> Shock electrons have been detected as peaks in angular distributions of low-energy electrons emitted from the ion beam exit side of thin foils.<sup>1,6-9</sup> Within a model which takes into account the refraction of electrons at the surface potential barrier, it has been predicted that it should even be possible to detect shock electrons in angular distributions of electrons emitted from the beam entrance side of thick solid samples.<sup>8</sup>

Recently, a possible influence of the superconducting phase transition on ion induced electron emission from high- $T_c$  superconductors has been reported.<sup>10</sup> Also, the question has been raised whether electron emission and, in particular, the collective emission of shock electrons is influenced by the superconducting phase transition.<sup>10-14</sup>

The discovery of the high-temperature superconductors<sup>15</sup> made it possible to test these considerations: we have performed first studies of secondary electron energy and angular distributions ( $0\text{ eV} \leq E \leq 40\text{ eV}$ ,  $25^\circ \leq \theta \leq 90^\circ$ ) from  $H^+$  and  $C^+$  (2 MeV) bombardment of single crystals of  $YBa_2Cu_3O_{7-\delta}$  and  $EuBa_2Cu_3O_{7-\delta}$  high- $T_c$  su-

perconductors at sample temperatures above ( $T = 300$  K) and below  $T = 35$  K) the superconducting transition temperature ( $T_c \approx 90$  K) as a function of the angle of incidence ( $\delta = 55^\circ, 65^\circ, 70^\circ, 75^\circ$ ) of the projectiles.  $\delta$  denotes the target tilt angle or the angle of incidence of the ions ( $\delta = 0^\circ$  means perpendicular ion impact).

Furthermore, the total yield  $\gamma_T$  of electrons induced by  $H^+$  and  $Ar^+$  (0.8 MeV) from polycrystalline  $YBa_2Cu_3O_{7-\delta}$  has been measured as a function of the probe temperature ( $70 \text{ K} \leq T \leq 300 \text{ K}$ ). We summarize experimental results on the influence of magnetic and structural phase transitions and, in particular, the superconducting phase transition at  $T = T_c$  on ion-induced electron emission from solids.

## II. EXPERIMENT

The electron energy and angular distributions presented here were measured with a new ultrahigh vacuum system at the 2.5-MV Van-de-Graaff-accelerator facility of the J. W. Goethe University in Frankfurt am Main.<sup>11</sup> A residual pressure of  $p < 7 \times 10^{-10}$  Torr was obtained with a cryopump.

A schematic drawing of the experimental setup is shown in Fig. 1. A  $45^\circ$  electrostatic parallel plate electron energy analyzer (electron spectrometer, energy resolution  $\Delta E/E \approx 3\%$ )<sup>16</sup> was used to record doubly differential electron energy spectra  $d^2n/dE d\Omega$  ( $0 \text{ eV} < E_e < 80 \text{ eV}$ ) at different observation angles  $\theta$  ( $25^\circ \leq \theta \leq 90^\circ$ ).  $\theta$  is measured with respect to the beam axis, i.e.,  $\theta = 0^\circ$  is the beam direction. The ion beam current was collected with a Faraday cup.

The targets were mounted on a copper sample holder connected to the coldhead of a closed-loop helium refrigerator with a copper rod. This cooling device is integrated in an *XYZ* manipulator with additional  $LN_2$  shielding. The target could be tilted with respect to the beam axis (tilt angle  $\delta$ ,  $0^\circ \leq \delta \leq 90^\circ$ ).  $\delta = 0^\circ$  means perpendicular ion impact, and the case where  $\delta$  approaches  $90^\circ$  is usually called "grazing incidence." With this novel equipment the target could be cooled to temperatures below  $T = 30$  K.

The electron yield data presented in Sec. VI have been obtained in a very simple way by measuring the ion-induced target current.<sup>17</sup> A negative potential of  $U = -30$  V was applied to the target to avoid influences due to contact or surface potentials (compare Refs. 1 and 10). In these experiments, polycrystalline  $YBa_2Cu_3O_{7-\delta}$  was used.<sup>10</sup> More details of the experimental setup are

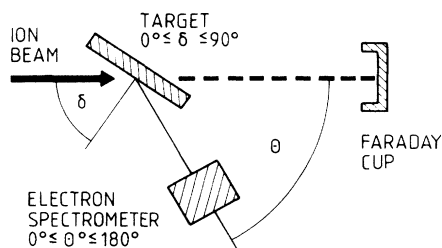


FIG. 1. Schematic drawing of the experimental setup.

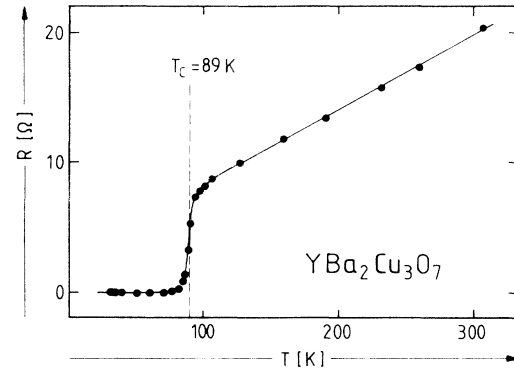


FIG. 2. Temperature dependence of the resistance  $R$  of a  $YBa_2Cu_3O_{7-\delta}$  film.

described elsewhere.<sup>11,16</sup>

It is difficult to prepare clean, well-defined surfaces of the ceramic high-temperature superconductors for spectroscopic investigations.<sup>18</sup> Standard methods for surface cleaning are, e.g., sputter-cleaning with heavy ions or heating of the probe (compare, e.g., Refs. 1, 8, 11, 19, and 20). Unfortunately, both methods lead to a destruction of the superconductor properties of the copper oxides either by radiation damage<sup>21</sup> or degassing of oxygen.<sup>15,18</sup> Recently, the method of *in situ* cleaving of the crystals has been used to obtain microscopically clean surfaces.<sup>22</sup>

Therefore, as a first approach, we used single crystalline thin  $YBa_2Cu_3O_{7-\delta}$ -films ( $d \approx 2000\text{--}3000$  Å) on  $SrTiO_3$ -substrate and  $EuBa_2Cu_3O_{7-\delta}$ -films on  $ZrO_2$ -substrate ( $d = 1$  mm,  $A = 10 \text{ mm} \times 5 \text{ mm}$ ) grown epitaxially by magnetron sputtering<sup>23</sup> as targets, because the surface of these films is of high quality with a disordered layer thickness as thin as  $d < 6$  Å. Even ultrathin films of  $d \approx 20$  Å prepared in this way showed three-dimensional superconducting behavior.<sup>23</sup> This approach is further justified by the fact that shock electrons have even been observed from uncleaned foil surfaces covered with about two monolayers of hydrocarbon adsorbates.<sup>7</sup> The single crystals are grown with the  $c$  axis perpendicular to the film plane, i.e., the  $CuO$  planes are parallel to the surface.

The resistance of the high- $T_c$  superconductor single-crystal film could be measured *in situ* by a standard four-point probe. A typical example of the temperature ( $T$ ) dependence of the resistance  $R$  of a  $YBa_2Cu_3O_{7-\delta}$  film is shown in Fig. 2. The linear dependence of  $R$  on  $T$  above  $T_c$  and the phase transition to superconductivity with  $R = 0$  at  $T = T_c \approx 89$  K can be observed. The ion fluence  $F$  was kept below  $F < 10^{13}$  ions/cm<sup>2</sup> to avoid a reduction of the superconducting transition temperature  $T_c$  by radiation damage.<sup>21</sup>

## III. ENERGY DISTRIBUTIONS

In Fig. 3 we present angle-integrated energy distributions  $N(E)$  from proton ( $H^+$ ) and heavy ion ( $C^+$ ) bombardment of  $YBa_2Cu_3O_{7-\delta}$  and  $EuBa_2Cu_3O_{7-\delta}$  (projectile energy  $E_p = 2$  MeV). They have been obtained by integrating doubly differential electron energy spectra

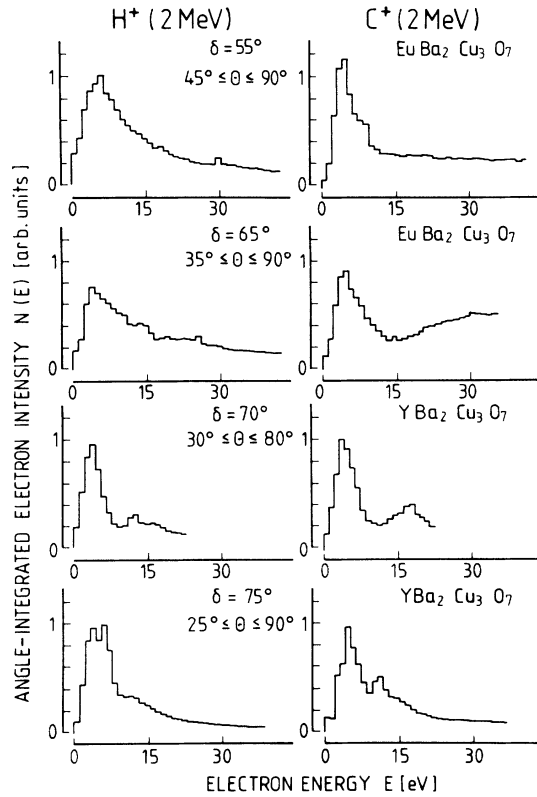


FIG. 3. Angle-integrated energy distributions  $N(E)$  from proton ( $H^+$ ) and heavy ion ( $C^+$ ) bombardment of  $YBa_2Cu_3O_{7-\delta}$  and  $EuBa_2Cu_3O_{7-\delta}$  (projectile energy  $E_p = 2$  MeV).

$d^2n/dE_e d\Omega$  taken at different observation angles  $\theta$  over the angular interval indicated in the figure.

In all the cases, the electron energy distributions from the high- $T_c$  superconductors show the characteristic low-energy "true secondary" electron maximum at  $E \approx 5$  eV.<sup>1,9,11,20</sup> No significant difference for proton and heavy ion impact can be observed. This may be a hint that the low-energy "true secondary" electron peak mainly consists of secondary electrons created by high-energy electrons in collision cascades (compare Refs. 1 and 24).

In the case of  $YBa_2Cu_3O_{7-\delta}$ , a further weak structure can be seen at  $E = 14 \pm 2$  eV. It is probably caused by Auger electron emission from yttrium. Both the intensity and the mean energy of this peak show a strong dependence on the observation angle  $\theta$ , but not on the type of projectile or the temperature. This can possibly be explained by directional effects<sup>25</sup> as discussed in the next section.

#### IV. ANGULAR DISTRIBUTIONS

It is well known that the (electronic) energy loss of ions in single crystals  $S(\delta)$  depends on the angle of incidence  $\delta$  of the projectiles, it will be reduced under channeling conditions. Since electron transport and transmission through the surface depend on the crystal structure, even for a fixed-ion impact angle  $\delta$  the intensity  $N(\theta)$  of elec-

trons from single crystals strongly depends on the emission angle  $\theta$  (or the observation angle  $\theta'$  measured with respect to the surface plane,  $\theta' = \theta + \delta - 90^\circ$ ),<sup>25</sup>

$$N(\theta) = \Lambda(\theta')S(\delta). \quad (1)$$

This is in contrast to the angular dependence of electron emission from polycrystalline samples, where the angular distribution of low-energy electrons roughly exhibits a cosine dependence<sup>1,24</sup>

$$N(\theta) \sim \cos\theta'. \quad (2)$$

This nonmonotonic behavior [Eq. (1)] and the deviation from the cosine law [Eq. (2)] is clearly demonstrated in Fig. 4, which shows the angular distributions  $N(\theta)$ , i.e., the electron intensities  $N$  as a function of the observation angle  $\theta$ , from  $H^+$  and  $C^+$  bombardment of  $YBa_2Cu_3O_{7-\delta}$ . All the angular distributions presented here have been obtained by integrating the doubly differential spectra  $d^2n/dE d\Omega$  over a certain energy interval  $\Delta E$  as indicated in the figures.

In the case of electron emission from single crystals, the nonmonotonic dependence of  $N(\theta)$  on  $\theta$  may shadow the possible shock electron peaks in electron angular distributions which are clearly visible for polycrystalline samples.<sup>1,6-9</sup> However, by comparing heavy  $C^+$  ion- ( $v_p = 2.6 v_B$ ) induced electron intensities to the fast proton- ( $v_p \approx 9 v_B$ ) induced electron intensities, i.e., by calculating the ratio

$$R(\theta) = N(C^+)/N(H^+), \quad (3)$$

we can account for the dependence of electron emission on the crystal orientation. The ratio  $R(\theta)$  should be a constant, i.e.,  $R(\theta) = R_0$  if the internal electron energy and angular distribution is independent of the projectile nuclear charge  $Z_p$ . Since the intensity of electron emission is roughly proportional to the electronic stopping power  $S(Z_p)$  of the swift ions,<sup>1,24,26</sup> the absolute value of  $R_0$  should be given by the ratio  $S(C^+)/S(H^+)$ , i.e.,

$$R(\theta) = R_0 = S(C^+)/S(H^+) \approx 10 \quad (4)$$

in the present case ( $E_p = 2$  MeV).<sup>27</sup>

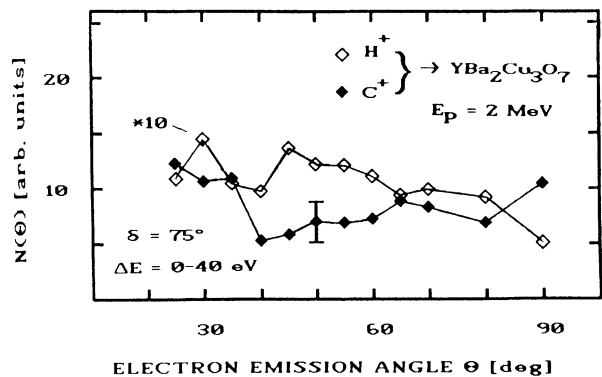


FIG. 4. Angular distributions  $N(\theta)$  of the electron intensities  $N$  as a function of the observation angle  $\theta$  from  $H^+$  and  $C^+$  bombardment of  $YBa_2Cu_3O_{7-\delta}$ .

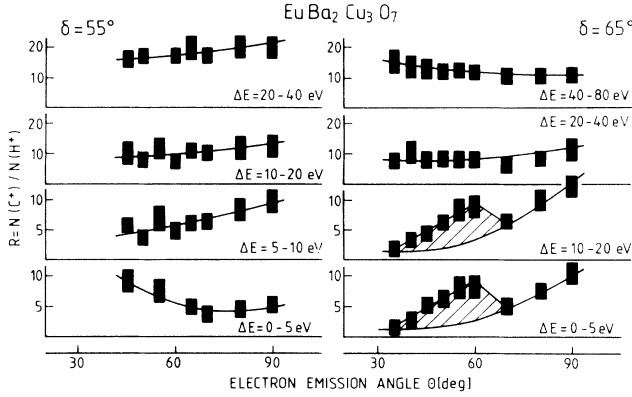


FIG. 5. Angular distributions of the electron intensity ratios  $R(\theta) = N(C^+)/N(H^+)$  from  $H^+$  and  $C^+$  (2 MeV) bombardment of single crystals of  $\text{EuBa}_2\text{Cu}_3\text{O}_7$  high- $T_c$  superconductors. The target tilt angles  $\delta$  and the energy intervals  $\Delta E$  are indicated in the figure. The width of the bars corresponds to the angular acceptance of the spectrometer, their height represents the error bar. The solid lines are drawn to guide the eye.

Nevertheless, deviations from this simple rule [Eq. (4)] are likely to occur because of possible deviations of heavy ion-induced electron angular distributions from proton induced ones, because of such phenomena as the contribution of lost projectile electrons,<sup>9</sup> screening of the projectile charge by the projectile electrons, excitation of the heavy ion's electrons, etc.<sup>1</sup> Enhancements due to an additional contribution to the electron intensity caused by the heavy ions should be visible as peaks in the angular distributions of the ratio  $R(\theta)$  as defined by Eq. (3).

Four sets of angular distributions of the ratio  $R(\theta)$  from high- $T_c$  superconductors single crystals taken at different target tilt angles  $\delta$  are shown in Fig. 5 ( $\text{YBa}_2\text{Cu}_3\text{O}_{7-\delta}$ ) and Fig. 6 ( $\text{EuBa}_2\text{Cu}_3\text{O}_{7-\delta}$ ). As can be expected from Eq. (4), the absolute value of the ratios  $R(\theta)$  is in an order of  $5 \leq R(\theta) \leq 15$ . At  $\delta = 55^\circ$ ,  $R(\theta)$  slightly increases with  $\theta$ , no structures can be observed over an electron energy range of  $5 \text{ eV} \leq E \leq 40 \text{ eV}$ . This slight increase may possibly be caused by the collisional loss of projectile electrons from the heavy  $C^+$  ions (see, e.g., Refs. 1 and 9).

Taking this slight increase at  $E < 20 \text{ eV}$  into account, surprisingly, the other three angular distributions ( $\delta = 65^\circ, 70^\circ$ , and  $75^\circ$ ) exhibit a broad peak ( $\Delta\theta \approx 25^\circ$ ) at low-electron energies  $E < 20 \text{ eV}$  at  $\delta$ -depending mean emission angles  $\theta_{em}$ . At higher energies  $E > 20 \text{ eV}$ , no other angular distribution shows such structures. Furthermore, an additional enhancement appears at  $25^\circ \leq \theta_{em} \leq 55^\circ$  in the energy interval  $10 \text{ eV} \leq E \leq 20 \text{ eV}$  for the highest tilt angle of  $\delta = 75^\circ$ .

The total widths of the regions of enhanced heavy ion-induced electron emission,  $\theta_{em}$  (black bars), at electron energies of  $0 \text{ eV} \leq E \leq 15 \text{ eV}$  for  $\delta = 65^\circ$ ,  $0 \text{ eV} \leq E \leq 20 \text{ eV}$  for  $\delta = 70^\circ$  and  $5 \text{ eV} \leq E \leq 10 \text{ eV}$  for  $\delta = 75^\circ$  are shown in Fig. 8 as a function of the target tilt angle  $\delta$ . Clearly, it can be seen that the mean emission angle  $\theta_{em}$  of the excess electrons belonging to the peaks at  $\theta_{em}$  shifts to higher angles  $\theta$  with increasing tilt angle  $\delta$ .

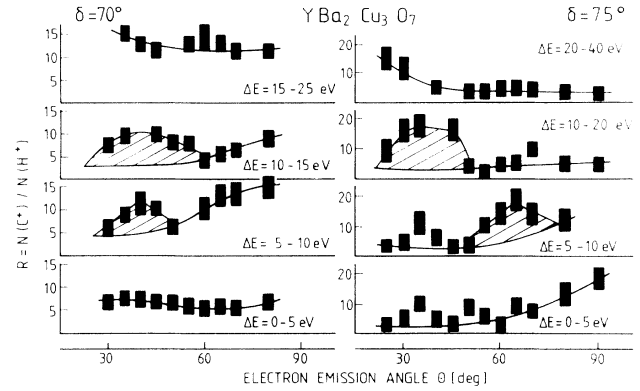


FIG. 6. Angular distributions of the electron intensity ratios  $R(\theta) = N(C^+)/N(H^+)$  from  $H^+$  and  $C^+$  (2 MeV) bombardment of single crystals of  $\text{YBa}_2\text{Cu}_3\text{O}_7$  high- $T_c$  superconductors. The target tilt angles  $\delta$  and the energy intervals  $\Delta E$  are indicated in the figure. The width of the bars corresponds to the angular acceptance of the spectrometer, their height represents the error bar. The solid lines are drawn to guide the eye.

## V. THE REFRACTION MODEL

The enhancement of heavy ion-induced electron emission and the dependence on the target tilt angle can be explained within the framework of a model for the refraction of low-energy electrons at surfaces. They are caused by the directed emission of shock electrons perpendicular to the conical shock wave of the charge density fluctuations induced by the ion wake.<sup>4-9</sup> Figure 7 explains the simple model. Shock electrons moving through the solid in a direction perpendicular to the wake shock front are refracted at the surface. Their velocity component perpendicular to the surface is reduced corresponding to the surface potential barrier  $U$ . It has been predicted<sup>8</sup> that the observable mean emission angle  $\theta_{em}^{exp}$  from the beam entrance side of the solid is then given by

$$\begin{aligned} \theta_{em}^{exp} &= f(\theta_{em}^{th}(v_p, \omega_p), U, E_s, \delta) \\ &= 180^\circ - \delta - \arcsin\left[\left(1 + \left(\frac{U}{E_s}\right)^{1/2}\right) \times \sin(180^\circ - \delta - \theta_{em}^{th})\right]. \end{aligned} \quad (5)$$

A detailed discussion is given in Refs. 1 and 8.

Under the (weak) assumption that the mean shock electron energy  $E_s$  and the surface potential barrier  $U$  are of the same order of magnitude, i.e.,  $U/E_s \approx 1$ , we can cal-

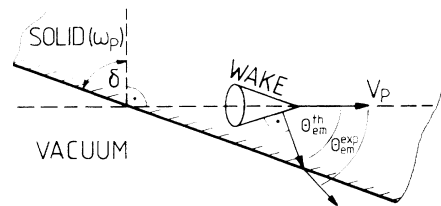


FIG. 7. Definition of the target tilt and electron-emission angle used for the calculation of the electron refraction by the surface potential.

culate the mean emission angle  $\theta_{em}^{exp}$  from Eq. (2) if the internal angle  $\theta_{em}^{th}(v_p, \omega_p)$  is known. Considering the plasma frequency  $\omega_p^{FC}$  of the free charge carriers (O  $2p$  holes) of the high- $T_c$  superconductors of the  $YBa_2Cu_3O_{7-\delta}$  type to be  $\hbar\omega_p^{FC} \approx 1.5$  eV,<sup>18</sup> we can estimate  $\theta_{em}^{th}(v_p, \omega_p)$  according to Ref. 4 and calculate  $\theta_{em}^{exp}$  under the assumption that the wake induced by a positively charged particle in a hole plasma resembles the wake induced by a negatively charged particle (e.g., an antiproton) in an electron plasma. In this case, the maxima and minima of the electron density fluctuations are exchanged, but the spatial structure and the internal angle  $\theta_{em}^{th}$  can be expected not to change strongly.<sup>3,4,13</sup>

The result of the calculation is shown in Fig. 8 in comparison to the experimental results. Within the experimental and theoretical uncertainties we find a reasonable agreement between the observed emission angles  $\theta_{em}$  (black bars) and the calculated mean emission angles  $\theta_{em}^{exp}$ . In particular, it is important to note that shock electron emission is not observed at  $\delta = 55^\circ$ , in agreement with the calculation according to Eq. (5). In this case, the shock electrons cannot overcome the surface potential barrier and are totally reflected when they arrive at the surface.

The peak appearing at  $25^\circ \leq \theta_{em} \leq 55^\circ$  in the energy interval  $10 \text{ eV} \leq E \leq 20 \text{ eV}$  for the highest tilt angle  $\delta = 75^\circ$  can be attributed to shock electron emission caused by collective excitation of all the electrons in one unit cell of the crystals with a volume plasma frequency of  $\hbar\omega_p^{VP} \approx 25$  eV.<sup>18</sup> The opening angle of the wake and thus the shock electron emission angle  $\theta_{em}$  only depend on the plasma frequency  $\hbar\omega_p$  (or, in other words, the density of the charge carriers  $n$ ) of the collective mode.<sup>3-4,7</sup>

At this point, it is important to note that emission of shock electrons by the protons of  $v_p \approx 9 v_B$  would lead to a reduction of the ratio  $R$  as defined by Eq. (4) at observation angles  $\theta_{em}(H, v_p \approx 9v_B) > \theta_{em}(C, v_p \approx 2.6v_B)$ . Thus, if shock electron emission can be observed both with protons and heavy ions, the typical dependence of the angular distributions  $R(\theta)$  on  $\theta$  should be characterized by a

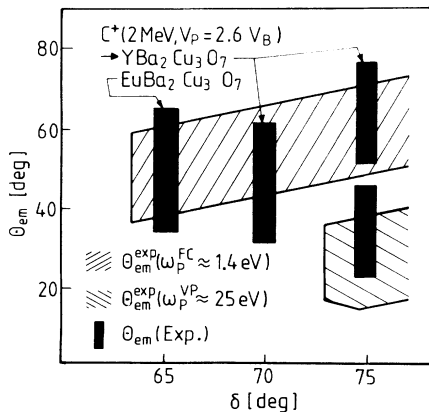


FIG. 8. Mean shock electron emission angle  $\theta_{em}$  as a function of the target tilt angle  $\delta$  (black bars). The theoretical prediction taking into account the refraction of low energy electrons at the surface for  $\theta_{em}^{exp}$  according to Eq. (2) is shown for comparison.

huge enhancement  $R > R_0$  at  $\theta_{em}(C, v_p \approx 2.6v_B)$  followed by a small dip at  $\theta_{em}(H, v_p \approx 9v_B) > \theta_{em}(C, v_p \approx 2.6v_B)$ . This is in agreement with the shape of the angular distributions shown in Figs. 5 and 6. However, since the intensity of shock electron emission decreases with increasing velocity and should scale with the square of the effective charge of the ions (compare Refs. 4-7), the effect of proton-induced shock electron emission can be expected to be negligible.

Although a first approach has been made, this experimental result could not yet be described by theory. Recent calculations on the wake in a two-component plasma characterized by two different plasma frequencies<sup>14</sup> showed that the oscillating part of the wake, i.e., the Mach shock wave, has only one component. Probably, the fact that the two collective resonances  $\omega_p^{FC}$  and  $\hbar\omega_p^{VP}$  of the high-temperature superconductors appear at quite different excitation energies of  $\sim 1$  eV and  $\approx 25$  eV may explain this discrepancy. The separation in energy causes a weak coupling of the two modes and thus leads to the appearance of two (nearly) independent components of the wake.<sup>28</sup> Each of them is characterized by a different opening angle and each leads to directed emission of shock electrons under a different angle.

## VI. THE SUPERCONDUCTING PHASE TRANSITION

The influence of phase transitions on the emission of secondary particles has been reviewed by Evdokimov.<sup>29</sup> As examples for the dependence of ion-induced electron emission on phase transitions appearing at a critical temperature  $T_c$ , we show in Fig. 9 the total electron yield  $\gamma_T$  as a function of the relative probe temperature  $T - T_c [K]$  for three different kinds of phase transitions. The ions species, their energy, the target, the kind of phase transi-

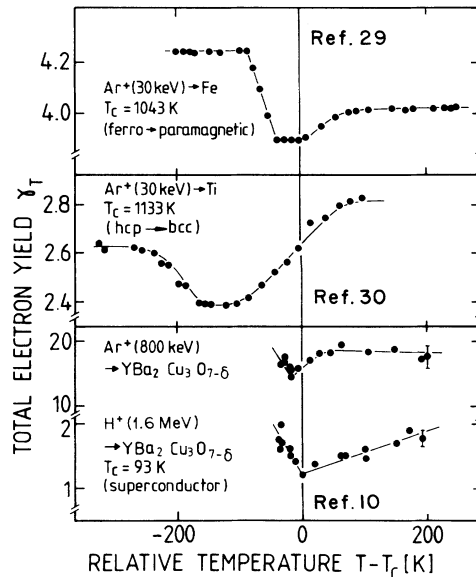


FIG. 9. Influence of phase transitions on the heavy-ion-induced secondary electron yield  $\gamma_T$ , which is plotted as a function of the relative probe temperature  $T - T_c$  (K).  $T_c$  denotes the critical temperature of the occurring phase transition.

tion, and the values of the corresponding critical temperatures are indicated in the figure.

The top of Fig. 9 shows  $\gamma_T(T-T_c)$  for polycrystalline Fe, which undergoes a phase transition from a ferromagnetic to a paramagnetic state (from Refs. 29 and 30). The middle of this figure shows  $\gamma_T(T-T_c)$  for the structural phase transition of Ti from the low-temperature hcp crystal structure to the high-temperature bcc structure.<sup>29</sup> The bottom of Fig. 9 presents  $\gamma_T(T-T_c)$  for the high-temperature copper oxide superconductor  $\text{YBa}_2\text{Cu}_3\text{O}_{7-\delta}$  (from Ref. 10).

It is interesting to note that all of the data sets shown exhibit a minimum of the electron yield  $\gamma_T$  close to the critical temperature  $T_c$ . The yields seem to be slightly different far above and below the critical temperature. Possibly, this behavior can be explained by a modification of the electron transport length or the surface potential barrier.<sup>10,29,30</sup> However, and in particular in the case of the superconductors, these experimental findings are not yet fully understood.

In order to investigate the possible dependence of shock electron emission on the superconducting phase transition,<sup>8,10,12</sup> we have compared angular distributions

$$C(\theta) = N(T=35 \text{ K})/N(T=110 \text{ K}) \quad (6)$$

from  $\text{C}^+$  impact measured far below (at  $T=35 \text{ K} < T_c$ ) and slightly above ( $T > T_c = 110 \text{ K}$ ). Such angular distributions taken at three different target tilt angles  $\delta$  are shown in Fig. 10. The regions of enhanced electron emission from Figs. 5 and 6 are indicated by arrows. Within experimental uncertainties, no significant dependence of the shock electron emission on the superconducting transition at  $T_c$  has been found. In accordance with the results shown in Fig. 9 (Ref. 10), the values of  $C$  are slightly enhanced, i.e.,  $C \approx 1.2$ .

However, one could speculate that the mean emission angle  $\theta_{\text{em}}$  should be different above and below the critical phase transition temperature  $T_c$ , in particular for the copper oxide superconductors. Within the BCS model of superconductivity,<sup>31</sup> a certain fraction of the charge carriers (density  $n$ ) leading to the metallic (linear) conductivity above  $T_c$  will form Cooper pairs (density  $n_c$ ) which carry the superconducting current. Their number  $\Gamma$  can

be estimated<sup>15,32</sup> from the ratio of the binding energy of the Cooper pairs, i.e., the energy gap  $\Delta$ , to the energy of the edge of the Fermi distribution, i.e., the Fermi energy  $E_F$ ,

$$\Gamma = n_c/n \approx 2\Delta/E_F. \quad (7)$$

For conventional superconductors with, say,  $E_F \approx 10 \text{ eV}$  and  $2\Delta \approx 10 \text{ meV}$ ,  $\Gamma$  is small ( $\Gamma \approx 10^{-3}$ ) thus leading to a negligible change of the charge carrier density  $n$ .

The situation may be completely different in the case of the copper oxide superconductors:<sup>15,32</sup> A rough estimate with  $E_F \approx 0.2 \text{ eV}$  and  $2\Delta \approx 20 \text{ meV}$  leads to a value of  $\Gamma \approx 0.1$ . It is even possible that  $\Gamma$  may be close to unity. This could lead to a reduction of the charge carrier density  $n$  and, consequently, to a reduction of the opening angle of the wake. Taking into account that the surface potential barrier  $U$  could also be reduced with decreasing  $n$ ,<sup>33</sup> both effects combined may lead to an enhancement of the shock electron emission angle  $\theta_{\text{em}}$  below  $T_c$ .

Indeed, closer inspection of Fig. 10 shows a significant enhancement  $C > 1$  for  $\delta = 65^\circ$  and  $\Delta E = 0-5 \text{ eV}$  and for  $\delta = 70^\circ$  and  $\Delta E = 10-15 \text{ eV}$ , i.e., there may be a slight shift of the mean emission angle  $\theta_{\text{em}}$  toward higher angles  $\theta$  below  $T_c$ . However, a simple estimate from Eqs. (5) and (7) shows that the enhancement should be in an order of magnitude of  $\Delta\theta \approx 0.1^\circ - 1^\circ$ . This is beyond the angular resolution of our experiment, and further experimental investigations are necessary.

## VII. CONCLUSIONS

We have investigated the phenomenon of kinetic ion-induced electron emission from high-temperature copper oxide superconductors. We have shown examples of the influence of magnetic and structural phase transitions and, in particular, the superconducting phase transition at  $T = T_c$  on ion-induced electron emission from solids. Furthermore, we have presented the studies of electron energy and angular distributions from  $\text{H}^+$ – and  $\text{C}^+$ – impact on single crystals of  $\text{YBa}_2\text{Cu}_3\text{O}_{7-\delta}$  high- $T_c$  superconductors.

As a main result, the angular distributions show shock electron emission from the excitation of the superconductors at two collective resonances  $\hbar\omega_p^{\text{FC}} \approx 1.5 \text{ eV}$  and  $\hbar\omega_p^{\text{VP}} \approx 25 \text{ eV}$ . Finally, we presented some new ideas concerning the possible dependence of collective shock electron emission on the superconducting phase transition.

Only very few studies on this interesting subject have been performed until today, and there is clearly a need for further work. In particular, a theoretical understanding of the observed phenomena would be desirable.

In conclusion, the spectroscopy of ion-induced electrons, and, in particular, the spectroscopy of shock electrons can be used to study the refraction of low energy electrons at solid surfaces. Also, phase transitions as well as the contribution of collective excitations to the electronic structure of solids can be investigated by means of charged particle induced electron emission.

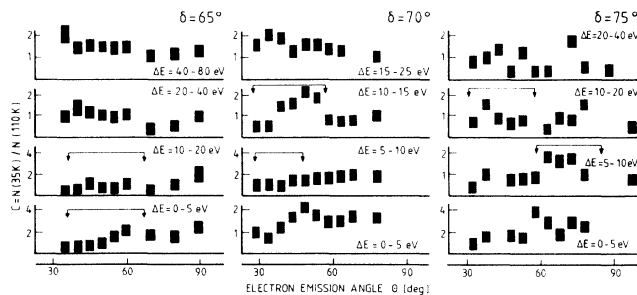


FIG. 10. Angular distributions of the ratio  $C$  of the integrated electron intensities below  $[N(35 \text{ K})]$  and above  $[N(110 \text{ K})]$  the critical phase transition temperature  $T_c$ . Four different energy intervals  $\Delta E$  are shown for each target tilt angle  $\delta$ .

## ACKNOWLEDGMENTS

We are grateful to O. Meyer and his colleagues for providing high-quality thin films of the high- $T_c$  superconductors. We would like to thank also P. M. Echenique, U. Gerhardt, W. Greiner, R. H. Ritchie, A. Schäfer, and

H. Stöcker for fruitful discussions and helpful suggestions. This work has been funded by the German "Bundesminister für Forschung und Technologie" (BMFT), Bonn, Germany, under Contract No. 06 OF 173/II Ti 476.

- \*Present address: Institut de Physique Nucléaire de Lyon, Groupe des Collisions Atomiques, Université Claude Bernard, 43 Bd. du 11 Novembre 1918, F-69622 Villeurbanne CEDEX, France.
- <sup>1</sup>For a recent extensive review of charged particle induced electron emission from solids, see D. Hasselkamp, H. Rothard, K. O. Groeneveld, J. Kemmler, P. Varga, and H. Winter, in *Particle Induced Electron Emission II*, edited by G. Höhler, E. A. Niekisch, and Springer Tracts in Modern Physics Vol. 123 J. Treusch, (Springer, Heidelberg, 1991). Theoretical aspects of the phenomenon are thoroughly discussed in J. Devooight, J. C. Dehaes, A. Dubus, M. Cailler, J. P. Ganachaud, M. Rössler, and W. Brauer, in *Particle Induced Electron Emission I*, edited by G. Höhler, E. A. Niekisch, (Springer Tracts in Modern Physics Vol. 122 J. Treusch, Springer, Heidelberg, 1991).
- <sup>2</sup>N. Bohr, *Mat. Fys. Medd. Dan. Vid. Selsk.* **18**, 8 (1948).
- <sup>3</sup>P. M. Echenique, R. H. Ritchie and W. Brandt, *Phys. Rev. B* **20**, 2567 (1979).
- <sup>4</sup>W. Schäfer, H. Stöcker, B. Müller, and W. Greiner, *Z. Phys. A* **288**, 349 (1978); *Z. Phys. B* **36**, 319 (1980).
- <sup>5</sup>D. K. Brice and P. Sigmund, *Mat. Fys. Medd. Dan. Vid. Selsk.* **40**, 8 (1980).
- <sup>6</sup>H. J. Frischkorn, K. O. Groeneveld, S. Schumann, R. Latz, G. Reichhard, J. Schader, W. Kronast, and R. Mann, *Phys. Lett.* **76A**, 155 (1980); H. J. Frischkorn, K. O. Groeneveld, S. Schumann, J. Schader, G. Astner, S. Hultberg, L. Lundin, R. Ramanujam, R. Didriksson, P. Hakansson, B. Sundquist, and R. Mann, in *Inner Shell and X-Ray Physics of Atoms and Solids*, edited by D. J. Fabian, H. Kleinpoppen, and L. M. Watsun (Plenum, New York, 1981), p. 193.
- <sup>7</sup>M. Burkhard, H. Rothard, C. Biedermann, J. Kemmler, K. Kroneberger, P. Koschar, O. Heil, and K. O. Groeneveld, *Phys. Rev. Lett.* **58**, 1773 (1987); H. Rothard, M. Burkhard, J. Kemmler, C. Biedermann, K. Kroneberger, P. Koschar, O. Heil, and K. O. Groeneveld, *J. Phys. (Paris)* **48**, C9-211 (1987).
- <sup>8</sup>H. Rothard, K. Kroneberger, M. Burkhard, C. Biedermann, J. Kemmler, O. Heil, and K. O. Groeneveld, *J. Phys. (Paris)*, **50**, C2-105 (1989).
- <sup>9</sup>Hermann Rothard, Kurt Kroneberger, Erling Veje, Markus Schosnig, Peter Lorenzen, Norman Keller, Jürgen Kemmler, Christoph Biedermann, Achim Albert, Oliver Heil, and Karl-Ontjes Groeneveld, *Nucl. Instrum. Methods B* **48**, 616 (1990).
- <sup>10</sup>H. Rothard, P. Lorenzen, N. Keller, O. Heil, D. Hofmann, J. Kemmler, K. Kroneberger, S. Lencinas, and K. O. Groeneveld, *Phys. Rev. B* **38**, 9224 (1988).
- <sup>11</sup>H. Rothard, M. Schosnig, K. Kroneberger, and K. O. Groeneveld, in *Interaction of Charged Particles with Solids and Surfaces*, edited by F. Flores, H. M. Urbassek, N. Arista, and A. Gras-Marti, NATO Advanced Study Institute, Alicante, Spain, 1990 (Plenum, New York, 1991).
- <sup>12</sup>K. Griepenkerl, B. Müller, and W. Greiner, *Radiat. Eff. Defects Solids* **110**, 215 (1989).
- <sup>13</sup>Hermann Rothard, Markus Schosnig, Dominik Schlösser, Kurt Kroneberger, Enio da Silveira, and Karl-Ontjes Groeneveld *Nucl. Instrum. Methods B* **56/57**, 843 (1991).
- <sup>14</sup>C. S. Warke, K. Griepenkerl, and W. Greiner, *Physica A* **170**, 248 (1991).
- <sup>15</sup>J. G. Bednorz and K. A. Müller, *Z. Phys. B* **64**, 189 (1986); *Rev. Mod. Phys.* **60**, 585 (1988).
- <sup>16</sup>W. Lotz, M. Burkhard, P. Koschar, J. Kemmler, H. Rothard, C. Biedermann, D. Hofmann, and K. O. Groeneveld, *Nucl. Instrum. Methods A* **245**, 560 (1986); M. Burkhard, W. Lotz, and K. O. Groeneveld, *J. Phys. E* **21**, 759 (1988).
- <sup>17</sup>J. Schader, B. Kolb, K. D. Sevier, and K. O. Groeneveld, *Nucl. Instrum. Methods* **151**, 563 (1978).
- <sup>18</sup>See, e.g., H. Romberg, N. Nücker, J. Fink, Th. Wolf, X. X. Xi, B. Koch, H. P. Geserich, M. Dürrler, W. Assmus, and B. Gegenheimer, *Z. Phys. B* **78**, 367 (1990); I. Bozovic, *Phys. Rev. B* **42**, 1969 (1990).
- <sup>19</sup>M. Burkhard, H. Rothard, J. Kemmler, K. Kroneberger, and K. O. Groeneveld, *J. Phys. D* **21**, 472 (1988a); P. Lorenzen, H. Rothard, K. Kroneberger, J. Kemmler, M. Burkhard, and K. O. Groeneveld, *Nucl. Instrum. Methods A* **282**, 213 (1989).
- <sup>20</sup>M. Schosnig, H. Rothard, K. Kroneberger, D. Schlösser, and K. O. Groeneveld, *Nucl. Instrum. Methods B* **68**, 394 (1992).
- <sup>21</sup>See, e.g., G. J. Clark, A. D. Marwick, P. H. Koch, and R. B. Laibowitz, *Appl. Phys. Lett.* **51**, 139 (1987); G. P. Summers, E. A. Burke, D. B. Chrisey, M. Nastasi, and J. R. Tesmer, *Appl. Phys. Lett.* **55**, 1469 (1989).
- <sup>22</sup>N. Schroeder *et al.* (unpublished).
- <sup>23</sup>J. Geerk, G. Linker, and O. Meyer, Kernforschungszentrum Karlsruhe GmbH Institut für Nukleare Festkörperphysik Report No. KfK-4601, 1989 (unpublished); X. X. Xi, G. Linker, O. Meyer, E. Nold, B. Obst, F. Ratzel, R. Smithey, B. Strehlau, F. Weschenfelder, and J. Geerk, *Z. Phys. B* **74**, 13 (1989).
- <sup>24</sup>J. Schou, *Scanning Microscopy* **2**, 607 (1988).
- <sup>25</sup>B. A. Brusilovsky, *Vacuum* **35**, 595 (1985).
- <sup>26</sup>H. Rothard, J. Schou, P. Koschar, and K. O. Groeneveld, *Nucl. Instrum. Methods B* **69**, 154 (1992).
- <sup>27</sup>J. F. Ziegler, J. P. Biersack, and U. Littmark, *The Stopping and Range of Ions in Matter* (Pergamon, New York, 1985).
- <sup>28</sup>P. M. Echenique and R. H. Ritchie (private communication).
- <sup>29</sup>I. N. Evdokimov, *Radiat. Eff.* **90**, 259 (1985).
- <sup>30</sup>I. N. Evdokimov and V. A. Molchanov, *Izvest. Akad. Nauk. SSSR* **33**, 762 (1969).
- <sup>31</sup>J. Bardeen, L. N. Cooper, and J. R. Schrieffer, *Phys. Rev.* **108**, 1175 (1957).
- <sup>32</sup>X. S. Guo, *Nucl. Instrum. Methods B* **45**, 698 (1990).
- <sup>33</sup>J. Hölzl and F. Schulte, in *Solid State Physics*, Springer Tracts in Modern Physics Vol. **85** (Springer, Heidelberg, 1979), p. 1.